Single buffer layers of $LaMnO_3$ or $La_{0.7}Sr_{0.3}MnO_3$ for the development of $YBa_2Cu_3O_{7-\delta}$-coated conductors: A comparative study

T. Aytug,[a] M. Paranthaman, H.Y. Zhai, H.M. Christen, S. Sathyamurthy, and D.K. Christen
Oak Ridge National Laboratory, Oak Ridge, Tennessee 37831

R.E. Ericson
3M Company, St. Paul, Minnesota 55144

(Received 27 March 2002; accepted 19 June 2002)

Single, epitaxial buffer layers of insulating $LaMnO_3$ (LMO) or conductive $La_{0.7}Sr_{0.3}MnO_3$ (LSMO) have been grown by sputter deposition on biaxially textured Ni and Ni–alloy substrates. We report baseline investigations of their compatibility with the $YBa_2Cu_3O_{7-\delta}$ (YBCO) coatings and demonstrate biaxially textured YBCO films grown by pulsed-laser deposition on these single-buffered tapes. Superconducting property characterizations revealed better properties for YBCO films on LMO-buffered tapes relative to those grown on LSMO layers. Self-field critical current densities (J_c) exceeding 1×10^6 A/cm^2 at 77 K have been obtained for the YBCO (200 nm) films on LMO-buffer layers. These results offer prospects for the use of single, LMO-buffered metal tapes in the development of practical YBCO-coated conductors.

Recently, good superconducting performance has been demonstrated in continuously processed, high-temperature superconducting (HTS) coated conductors on the basis of the approach of rolling-assisted biaxially textured metal substrates (RABiTS).[1,2] The RABiTS technique utilizes the biaxial texture of the metal substrate produced by thermomechanical processing[2] as a template for the epitaxial deposition of one or more buffer layers. This buffer then provides a structural template and a chemical barrier for the subsequent epitaxial growth of a HTS coating. Presently, the RABiTS-based coated conductors use Ni or dilute Ni–alloys as the tape substrates. These templates impart sufficient crystalline texture to the HTS material to ameliorate the pervasive problem of weak-linked, high-angle grain boundaries.[3,4]

Potential applications of HTS-coated conductors involve the efficient production, distribution, and storage of electrical power. Ideally, for these applications conductive-oxide buffer layers are preferred, since they can provide electrical coupling between the thin HTS layer and the thick underlying metal substrate, thereby improving the electrical and thermal stability of the structure against a transient to the dissipative regime. To date, however, developed buffer layers have comprised insulating oxides and multilayers.[1,2,5–7] Previously, high-quality $YBa_2Cu_3O_{7-\delta}$ (YBCO) films have been grown reproducibly on the RABiTS standard architecture of CeO_2/YSZ/CeO_2–(or Y_2O_3)/Ni.[2,5–6] Development of conductive-oxide buffer layers on RABiTS has begun recently with the demonstration of an epitaxial $SrRuO_3$/$LaNiO_3$ bilayer structure on Ni tapes.[8] The YBCO coatings deposited on the $SrRuO_3$/$LaNiO_3$/Ni architecture exhibited good electrical connectivity over the entire structure and yielded critical current density (J_c) values (at 77 K, self-field) exceeding 1.2×10^6 A/cm^2.

The fabrication of these multilayered buffer architectures however, presents major challenges. Generally, deposition of a complete buffer-layer sequence involves a combination of vacuum deposition techniques[1–8] and exposure of samples to multiple intermediate thermal cyclings and ambient environment. These requirements adversely affect the structural and chemical integrity of all individual sublayers and increase the overall process complexity. To overcome these difficulties, it is important to develop a single buffer layer, ideally conductive, that can be fabricated by an easily scalable deposition technique. Recently, we investigated viability of the doped rare earth manganate compound $La_{0.7}Sr_{0.3}MnO_3$ (LSMO) as a buffer layer for YBCO-coated conductors, due to its electrical conductivity, good thermal stability, and structural compatibility with YBCO.[9] In that study, YBCO films deposited on highly textured LSMO buffer layers on Ni tapes showed superconducting transition temperatures (T_c = 87–89 K) and J_c (77 K, self-field) values $\approx 5 \times 10^5$ A/cm^2. These values are somewhat

[a]e-mail: aytugt@ornl.gov

depressed compared to those obtained on either the standard CeO_2/YSZ/CeO_2–(or Y_2O_3)/Ni or the conductive $SrRuO_3$/$LaNiO_3$/Ni structure [T_c = 90–92 K, J_c (77 K) $\geq 1 \times 10^6$ A/cm^2]. The reason for this slight degradation was attributed to low-level Sr contamination of YBCO from the LSMO layers, as documented by secondary ion mass spectroscopy (SIMS). In light of the above observations, it is reasonable that the parent compound $LaMnO_3$ (LMO), if fabricated epitaxially on Ni and/or Ni–alloy, would resolve the Sr-contamination issue. While LMO is a semiconducting perovskite oxide, not a conductive buffer layer as LSMO, its pseudocubic lattice parameter (3.91 Å) is closely matched to that of the orthorhombic YBCO (3.86 Å). These characteristics point to possible viability as a single buffer layer for YBCO-coated conductors.

Here we report for the first time the growth of YBCO coatings on a single buffer layer with J_c (77 K) values above 1×10^6 A/cm^2, deposited both on biaxially textured Ni and on mechanically strengthened Ni–(3 at.% W–1.7 at.% Fe) alloy (referred to as Ni–alloy). A comparative study of the chemical compatibility and the superconducting properties (T_c, J_c) of YBCO films grown on single layers of both LSMO- and LMO-buffered Ni and Ni–alloy tapes is presented.

Biaxially textured Ni (99.99%) and Ni–alloy substrates were obtained by progressive cold rolling of polycrystalline, randomly oriented Ni and Ni–alloy bars, followed by a texturing anneal at 1100 °C (for pure Ni) and 1250 °C (for Ni–alloy). The 1-h heat treatment in a reducing, forming gas (96% Ar + 4% H_2) atmosphere yielded the desired (100) cube texture. Depositions of the LSMO and LMO buffer layers were conducted with an rf-magnetron sputtering system. The sputter targets were made from single-phase LSMO and LMO powders, prepared by solid-state synthesis, and lightly packed into a copper target tray. Typical sputtering conditions consisted of a sputter-gas mixture of forming gas and $(2–5) \times 10^{-5}$ torr of H_2O at a total pressure of 3 m torr. Substrate temperatures were in the range of 575–625 °C. Water vapor provided oxygen for the stability of the oxides and forming gas helped suppress the oxidation of the metal tapes. The LMO film thickness was varied in the range of 60 to 300 nm to investigate the effect on microstructure and on the superconducting properties of the subsequent HTS layer. The thickness of LSMO layers was maintained at around 300 nm. The deposition rate for both buffer materials using our laboratory equipment was approximately 0.56 Å/s.

The YBCO films were grown by pulsed laser deposition (PLD), using a KrF excimer laser system operated at an energy density of approximately 2 J/cm^2 and a repetition rate of 15 Hz. During YBCO deposition, the substrates were maintained at 780 °C in 120 mtorr of O_2. After deposition, the samples were first cooled to 500 °C at a rate of 5 °C/min; then the O_2 pressure was increased to 550 torr, and the samples were cooled to room temperature at the same rate. Typical YBCO film thicknesses were 200 nm. Crystal structures were characterized with a Philips model XRG3100 x-ray diffractometer (XRD), and microstructural analyses were conducted on a JOEL model, JSM-840 scanning electron microscope (SEM). SIMS depth–profile analyses were made to document possible cation contamination of YBCO. Electrical property characterizations were made using a standard four-probe technique on samples with dimensions of 15 mm in length and 5 mm in width, with values of J_c assigned at a 1-μV/cm criterion.

A typical XRD θ–2θ scan for a 300-nm-thick LMO layer deposited on biaxially textured Ni is given in Fig. 1, with the inset showing a logarithmic-scale (111) pole figure of the same LMO film. The presence of only (00*l*) reflections indicates that LMO is oriented with its *c* axis normal to the plane of the substrate, and the pole figure reveals a single-domain epitaxy, with the in-plane LMO[110]//substrate[110]. The ω-scan rocking curve on the LMO(002) and ϕ scan on the LMO(111) have yielded out-of-plane and in-plane peak-width full width at half-maximum of $\Delta\omega = 9°$ and $\Delta\phi = 10°$, respectively. Both distribution widths are comparable to those of the underlying Ni ($\Delta\omega = 9.4°$ and $\Delta\phi = 9.8°$) substrate. Similar crystallographic relations were observed for the growth behavior of LMO films on Ni–alloy tapes.

In addition to excellent crystalline quality, LMO layers show a crack-free, homogeneous, and dense microstructure. This point is displayed in Figs. 2(a) and 2(b), which show grain boundary regions for 300-nm-thick LMO-buffered Ni and Ni–alloy substrates. Similar surface morphologies were observed for films deposited at various thicknesses ranging from 60 to 300 nm. Figures 2(c) and 2(d) show typical surface morphologies of two YBCO films deposited on LMO(300 nm)/Ni and LMO(300 nm)/Ni–alloy substrates, respectively, where dense and

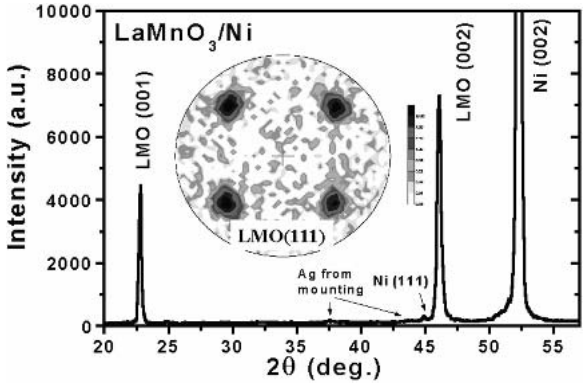

FIG. 1. Typical XRD θ–2θ pattern for a 300-nm-thick LMO buffer layer on biaxially textured Ni substrates. The inset shows a (111) logarithmic-scale pole figure of the same film.

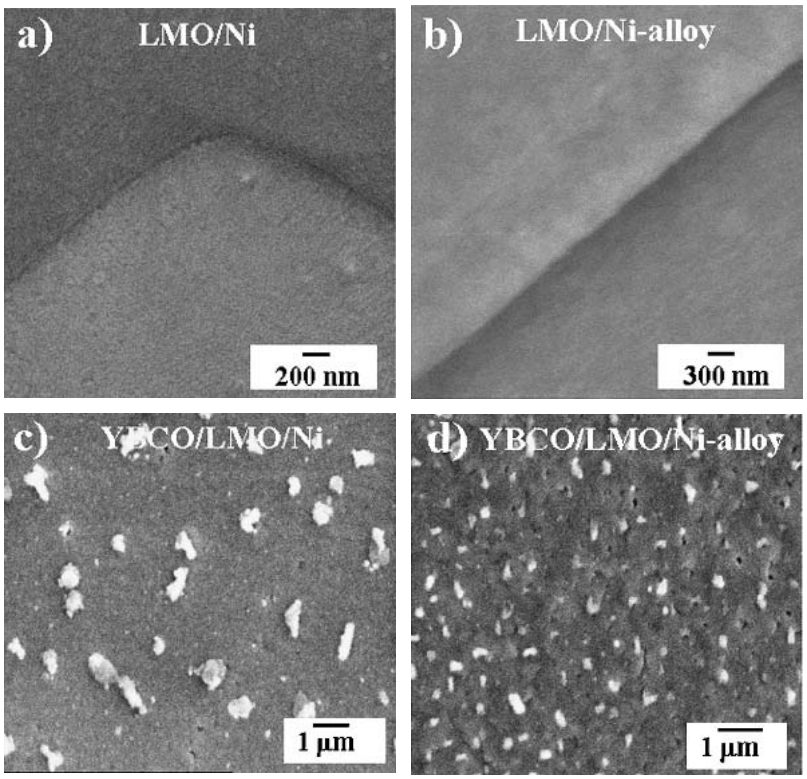

FIG. 2. SEM micrographs of 300-nm-thick LMO films deposited directly on biaxially textured (a) Ni and (b) Ni–alloy substrates and the surface morphology of YBCO film grown on LMO-buffered (c) Ni and (d) Ni–alloy tapes.

uniform microstructures are also observed. Overall, these results on LMO layers are very similar to those previously observed on the LSMO layers.[9]

The qualifying test for the suitability of any buffer layer structure on any metal tape is chemical compatibility with the YBCO coatings. Figures 3(a) and 3(b) compare the results of SIMS depth profile measurements on YBCO/LSMO/Ni and YBCO/LMO/Ni, respectively. Both samples show well-resolved interfaces and well-defined layers and effectively block Ni diffusion to within a thickness of few hundred angstroms, as evidenced by the sharp increase of the Ni signal near the buffer–substrate interface. For the YBCO/LSMO/Ni structure [Fig. 3(a)], the La and Mn signals remain at the noise level, while a significant broadening of the Sr signal within the YBCO layer indicates contamination. On the other hand, Fig. 3(b) clearly shows a cation contamination-free YBCO coating on the LMO/Ni structure. In fact, these SIMS results are in accordance with the differences observed in the electrical and superconducting properties of YBCO films deposited on LSMO[9] or LMO buffer layers. In Fig. 4, we compare the magnetic field dependence ($H \| c$ axis) of the transport J_c at 77 K for YBCO films deposited on LMO/Ni–(Ni–alloy) with those on LSMO/Ni–(Ni–alloy) architectures. To observe the effect of LMO thickness on the superconducting

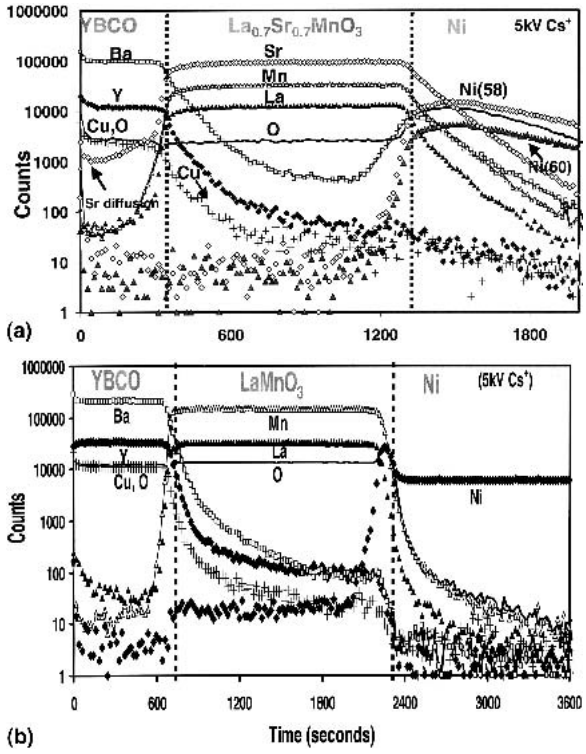

FIG. 3. SIMS depth profiles for (a) YBCO/LSMO/Ni and (b) YBCO/LMO/Ni multilayer structures.

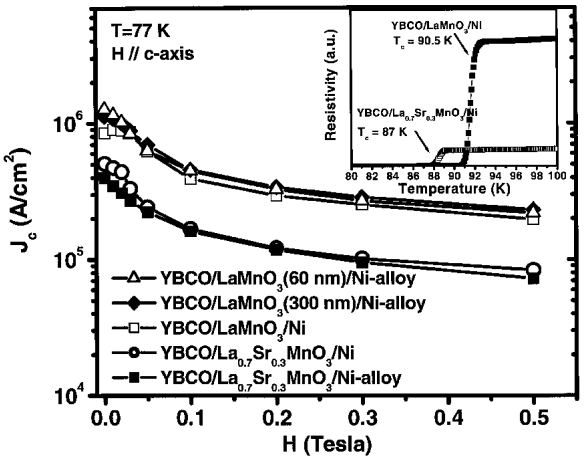

FIG. 4. Magnetic field dependence of J_c, measured at 77 K, for the YBCO films on LMO-buffered Ni and Ni–alloy substrates. Also shown for comparison are typical J_c (H, 77 K) data for YBCO/LSMO/Ni and YBCO/LSMO/Ni–alloy tapes. The inset shows the resistive superconducting transition region of the same YBCO/LMO/Ni and YBCO/LSMO/Ni structures.

properties of YBCO layers, we also present the J_c–H behavior of two samples having 60- and 300-nm-thick LMO layers. At zero applied field, YBCO films of thickness approximately 200 nm grown on LMO support high-$J_c \geq 1.0 \times 10^6$ A/cm^2, whereas the YBCO films on LSMO show approximately ½ that value. The transport properties are largely independent of LMO thickness in the range of 60–300 nm. Specifically, the self-field J_c of the YBCO/LMO(60 nm)/Ni–alloy is above 1.2×10^6 A/cm^2, which is comparable to the best J_c values obtained on RABiTS having both the "standard trilayer insulating" buffer architecture, CeO_2/YSZ/CeO_2–(or Y_2O_3)/Ni, and "bilayer conductive" architecture, $SrRuO_3$/$LaNiO_3$. The present results establish a new benchmark for performance since they were attained on a RABiTS structure having a single buffer layer. The inset of Fig. 4 shows the superconducting transition region of the temperature-dependent resistivity curves for the same YBCO/LMO/Ni and YBCO/LSMO/Ni samples. Differences in the net resistivity values between two samples are due to the electrical coupling between the HTS layer and the metal substrate through the conductive LSMO layer, providing an overall reduced resistivity. While the YBCO/LSMO/Ni exhibits a T_c of only 82 K, that of the YBCO/LMO/Ni structure is 90 K, further supporting a low-level of Sr contamination from the LSMO layer. It is well documented that Sr impurities in the superconducting structure can significantly reduce T_c.[10,11] This conclusion is also consistent with the lower J_c values observed for the YBCO films on LSMO layers.[9]

In summary, we have made a comparative study of the chemical compatibility and superconducting properties (T_c, J_c) of YBCO films grown on single layers of $La_{0.7}Sr_{0.3}MnO_3$(LSMO) and $LaMnO_3$(LMO) buffered biaxially textured Ni and Ni–alloy substrates. Although YBCO films on both buffers have good crystalline structure, the T_c and J_c of the YBCO on LMO layers have shown significantly higher values than those of the YBCO films grown on LSMO layers. These results are observed to be in accordance with the low-level Sr contamination of the YBCO originating from the LSMO layers. Our results also indicated that the LMO layer thicknesses in the range of 60–300 nm do not significantly effect the superconducting properties of the YBCO coatings. For epitaxial YBCO films on LMO/Ni–(Ni–alloy) tapes, typical self-field J_c(77 K) values of 1×10^6 A/cm^2 have been achieved. The present results provide initial support for implementation of LMO buffer layers in the development of second-generation HTS wires on the basis of the RABiTS approach to YBCO-coated conductors.

ACKNOWLEDGMENTS

This work was supported by the United States Department of Energy, Division of Materials Sciences, Office of Science, Office of Power Technologies-Superconductivity Program, and Office of Energy Efficiency and Renewable Energy. The research was performed at the Oak Ridge National Laboratory, managed by U.T.-Battelle, LLC, for the United States Department of Energy under Contract No. DE-AC05-00OR22725.

REFERENCES

1. D.P. Norton, A. Goyal, J.D. Budai, D.K. Christen, D.M. Kroeger, E.D. Specht, Q. He, B. Saffian, M. Paranthaman, C.E. Kalbunde, D.F. Lee, B.C. Sales, and F.A. List, Science **274,** 755 (1996).
2. A. Goyal, R. Feenstra, F.A. List, M. Paranthaman, D.F. Lee, D.M. Kroeger, D.B. Beach, J.S. Morell, T.G. Chirayil, D.T. Verebelyi, X. Cui, E.D. Specht, D.K. Christen, and P.M. Martin, J. Met. 19 (July 1999).
3. D. Dimos, P. Chaudari, J. Mannhart, and F.K. Legoues, Phys. Rev. Lett. **61,** 219 (1988).
4. D.T. Verebelyi, D.K. Christen, R. Feenstra, C. Cantoni, D.F. Lee, M. Paranthaman, P.N. Arendt, R.F. DePaula, J.R. Groves, and C. Prouteau, App. Phys. Lett. **76,** 1755 (2000).
5. M. Paranthaman, A. Goyal, F.A. List, E.D. Specht, D.F. Lee, P.M. Martin, Q. He, D.K. Christen, D.P. Norton, J.D. Budai, and D.M. Kroeger, Physica C **275,** 266 (1997).
6. F.A. List, A. Goyal, M. Paranthaman, D.P. Norton, E.D. Specht, D.F. Lee, and D.M. Kroeger, Physica C **302,** 87 (1998).
7. Q. He, D.K. Christen, R. Feenstra, D.P. Norton, M. Paranthaman, E.D. Specht, D.F. Lee, A. Goyal, and D.M. Kroeger, Physica C **314,** 105 (1999).
8. T. Aytug, B.W. Kang, C. Cantoni, E.D. Specht, M. Paranthaman, A. Goyal, D.T. Verebelyi, D.K. Christen, J.Z. Wu, R.E. Ericson, C.L. Thomas, C-Y. Yang, and S.E. Babcock, J. Mater. Res. **16,** 2661 (2001).
9. T. Aytug, M. Paranthaman, B.W. Kang, S. Sathyamurthy, A. Goyal, and D.K. Christen. Appl. Phys. Lett. **79,** 2205 (2001).
10. M. Oda, T. Murakami, Y. Enomoto, and M. Suziki, Jpn. J. Appl. Phys. **26,** L804 (1987).
11. T. Wada, S. Adachi, T. Mihara, and R. Inaba, Jpn. J. Appl. Phys. **26,** L706 (1987).